



Contents lists available at ScienceDirect

Genomics

journal homepage: www.elsevier.com/locate/ygeno

Q1 Identification of protein-interacting nucleotides in a RNA sequence using 2 composition profile of tri-nucleotides

Q2 Bharat Panwar¹, Gajendra P.S. Raghava^{*}

4 Bioinformatics Centre, CSIR-Institute of Microbial Technology, Sector 39A, Chandigarh, India

5 A R T I C L E I N F O

6 Article history:

7 Received 2 April 2014

8 Accepted 23 January 2015

9 Available online xxxx

10 Keywords:

11 Protein-interacting nucleotide (PIN)

12 Binary profile of patterns (BPP)

13 Tri-nucleotide composition profile of patterns

14 (TNCPP)

15 SVM

16 Prediction

17 RNApin

30 A B S T R A C T

The RNA–protein interactions play a diverse role in the cells, thus identification of RNA–protein interface is essential for the biologist to understand their function. In the past, several methods have been developed for predicting RNA interacting residues in proteins, but limited efforts have been made for the identification of protein-interacting nucleotides in RNAs. In order to discriminate protein-interacting and non-interacting nucleotides, we used various classifiers (NaiveBayes, NaiveBayesMultinomial, BayesNet, ComplementNaiveBayes, MultilayerPerceptron, J48, SMO, RandomForest, SMO and SVM^{light}) for prediction model development using various features and achieved highest 83.92% sensitivity, 84.82 specificity, 84.62% accuracy and 0.62 Matthew's correlation coefficient by SVM^{light} based models. We observed that certain tri-nucleotides like ACA, ACC, AGA, CAC, CCA, GAG, UGA, and UUU preferred in protein-interaction. All the models have been developed using a non-redundant dataset and are evaluated using five-fold cross validation technique. A web-server called RNApin has been developed for the scientific community (<http://crdd.osdd.net/raghava/rnapi/>).

© 2015 Published by Elsevier Inc.

32 Q4 1. Introduction

The interaction of RNA molecules and RNA-binding proteins (RBPs) play diverse roles in cells including protein translation, gene expression and regulation [1]. There is a large amount of RNA present in every cell, but these RBPs are selectively bound to the particular RNA at a specific site [2,3,4]. Role of RNA–protein interactions is well established for the complete functionality of cell, and in the case of its failure, this leads to the various human genetic diseases [5] such as fragile X syndrome [6], paraneoplastic neurologic syndromes [7], spinal muscular atrophy [8], myotonic dystrophy [9] and fragile X tremor ataxia syndrome [10].

Detection of protein interacting nucleotides is important to understand the underlying mechanism of RNA–protein interaction. X-ray crystal structure determination of RNA–protein complexes is a common practice to detect PINs in RNA but structural availability of these complexes is very low in comparison to total protein interacting RNAs. There are several other experimental techniques such as RNA EMSA [11], SELEX (systemic evolution of ligands exponential enrichment), CLIP [12], pull-down assay, oligonucleotide-targeted RNase H protection assays [13], RIP–CHIP [14], ribonomics [15] and Ribotrap [16] available for the detection of protein binding RNAs. These techniques are

expensive, laborious and unable to provide exact information of protein interacting nucleotides. In the past, several methods have been developed for the prediction of RNA interacting residues (amino acids) in the protein sequences [17,18,19,20] but limited efforts have been made for predicting protein interacting nucleotides (PINs) in the RNA sequences [21]. Therefore, there is an urgent need to develop computational tool for this problem.

Recently, many studies have suggested important steps to develop any biological prediction method [22,23,24,25,26,27,28]. In this study a systematic attempt has been made to develop in silico tool for the prediction of PINs in RNA sequences. We analyzed the patterns of both protein interacting and non-interacting nucleotides and found that significant differences were present. A machine learning technique 'support vector machine' has been applied. We used different binary and compositional approaches and achieved highest 0.62 MCC and 0.889 AUC by tri-nucleotide composition profile of patterns (TNCPP) approach. In order to provide service to the global scientific community, this TNCPP based prediction model has been implemented in the form of a web-server called RNApin.

2. Material and methods

2.1. Datasets

We retrieved a total of 1546 protein-interacting RNA chains (RNA–1546) of PDB from PRIDB database [29]. We used these RNA chains and created 25% non-redundant 'RNA-208' dataset of 208 RNA chains using BLASTCLUST software. We considered only RNA chains having

* Corresponding author at: Bioinformatics Centre, Institute of Microbial Technology, Sector 39A, Chandigarh, India. Fax: +91 172 2690632, 2690585.

E-mail addresses: bharat@imtech.res.in (B. Panwar), raghava@imtech.res.in (G.P.S. Raghava).

URL: <http://www.imtech.res.in/raghava/> (G.P.S. Raghava).

¹ Present address: Department of Computational Medicine Bioinformatics, University of Michigan, Ann Arbor, MI 48,109, USA.

length of more than 10 nucleotides. Furthermore, we assigned each nucleotide of these RNA chains into protein interacting and non-interacting nucleotides using cutoff distance of 5.0 cutoff Å. It means that if the distance between nucleotide and any amino acid of protein chains was less or equal than 5.0 Å, then nucleotide assigned as protein interacting otherwise is assigned as non-interacting. In this way, we assigned a total of 46,582 nucleotides of RNA-208 dataset into the 10,198 protein interacting and 36,384 non-interacting nucleotides. We used 5.0 Å as cut-off because this contains almost all different kind of interactions and mostly used in the past for the prediction of RNA-interacting amino acids [30].

2.2. Creation of sliding window

In the past, sliding (overlapping) window based strategy has been applied in various residue/nucleotide level prediction methods [20,31,17]. In this study, we also created sliding window patterns of different 3–25 lengths from RNA-208 dataset. If the central nucleotide of the window was protein-interacting then whole window pattern was considered as positive pattern otherwise considered as negative patterns [32]. To generate fixed length window size of terminal nucleotides, we added a dummy 'X' nucleotide at both terminals of each RNA chain. The number of dummy nucleotides was calculated with $(L - 1) / 2$ formula (where L is the length of the pattern). It means that each nucleotide of RNA-208 dataset was once used at the central position of window pattern. Finally, we created a total of 10,198 positive and 36,384 negative patterns.

2.3. Binary profile of patterns

The numerical representation of window patterns is necessary for the machine learning tools, and BPP based strategy is one of the widely adopted approach for the window-based machine learning [31]. In BPP approach, we represented A, C, G, U and X nucleotides of all window patterns in the binary form of {1,0,0,0,0}, {0,1,0,0,0}, {0,0,1,0,0}, {0,0,0,1,0} and {0,0,0,0,1} respectively. BPP generated five times higher input features than the window size (e.g. 19-nucleotide long window pattern generates a total of 95 (19×5) input features). These binary representations of window pattern give information of nucleotide availability at a specific position during machine learning based prediction model development.

2.4. Composition profile of patterns

The composition of window pattern can also be used as input feature of machine learning [33,34].

2.4.1. Mono-nucleotide composition profile of patterns

In MNCP, we calculated mono-nucleotide composition of all nucleotides (A, C, G, U and X) for each window pattern separately. These five numerical values of composition were used as SVM input.

2.4.2. Di-nucleotide composition profile of patterns

In DNCPP, the di-nucleotide (AA, AC, AG, CG, AU, ..., XX) composition of each window pattern was calculated separately. It provided a total of 25 numerical values, which were used as SVM input. The DNCPP approach has advancement over MNCP and that it also provides information of neighboring nucleotides.

2.4.3. Tri-nucleotide composition profile of patterns

In TNCP, we calculated tri-nucleotide (AAA, AAC, AAG, ..., XXX) composition of each window pattern separately. For each window pattern, we found a total of 125 numerical values, which were used as SVM input features.

2.5. Support vector machine

In this study, a machine learning technique, support vector machine (SVM) was applied, which is based on the structural risk minimization principle of statistics learning theory. SVMs are a set of related supervised learning methods used for classification and regression mode [35]. It has options of different parameters and kernels (e.g. linear, polynomial, radial basis function and sigmoidal) to optimize according to need. We implemented SVM^{light} Version 6.02 package [36] of SVM and machine learning. We applied various parameters and three different (linear, polynomial and radial basis function) kernels to develop different prediction models.

2.6. WEKA

WEKA is a single package and platform of different classifier [37]. We applied WEKA 3.6.6 version, which consists of different classifiers such as NaiveBayes, NaiveBayesMultinomial, BayesNet, ComplementNaiveBayes, MultilayerPerceptron, J48, SMO, RandomForest and SMO. We have used all these machine learning algorithms for the development of different prediction models.

2.7. Five-fold cross validation

The validation of the model is an important step for the development of any prediction method. There are several techniques available for validation of any prediction models like jack-knife test or leave-one-out cross validation (LOOCV), n-fold cross validation etc. [38]. Although, jackknife or LOOCV cross-validation is the most objective and consistent, but it is time-consuming especially for the residue-level prediction [17,25,39]. In this study, we used widely accepted five-fold cross-validation technique for training, testing and evaluation of SVM models [40,41]. In this process, first we divided all positive and negative window patterns into five parts randomly. Each of these five sets consists of one-fifth of total positive and one-fifth of total negative window patterns. In five-fold cross validation technique, we used four sets as training and the remaining one set as testing. This process was repeated five times in such a way that each set was used once as a test set. We calculated performance of each test set and overall performance of the prediction model is an overall performance of these five test sets.

2.8. Evaluation parameters

We used various evaluation parameters such as sensitivity (Eq. (1)), specificity (Eq. (2)), accuracy (Eq. (3)) and MCC (Eq. (4)) values for evaluating prediction models [42]:

$$\text{Sensitivity} = \frac{TP}{TP + FN} \times 100 \quad (1)$$

$$\text{Specificity} = \frac{TN}{TN + FP} \times 100 \quad (2)$$

$$\text{Accuracy} = \frac{TP + TN}{TP + FP + TN + FN} \times 100 \quad (3)$$

$$\text{MCC} = \frac{(TP)(TN) - (FP)(FN)}{\sqrt{[TP + FP][TP + FN][TN + FP][TN + FN]}} \quad (4)$$

where TP, TN, FP and FN are True Positives, True Negative, False Positives and False Negatives respectively.

The above-mentioned parameters are threshold-dependent; therefore, we also calculated threshold-independent evaluation parameter, AUC (Area Under Curve) values for each prediction model in the ROC (Receiver Operating Curve) plots. The RNaPin web-server provides prediction results by calculating probability score for each nucleotide of the given RNA sequence. In order to present SVM score effectively, we

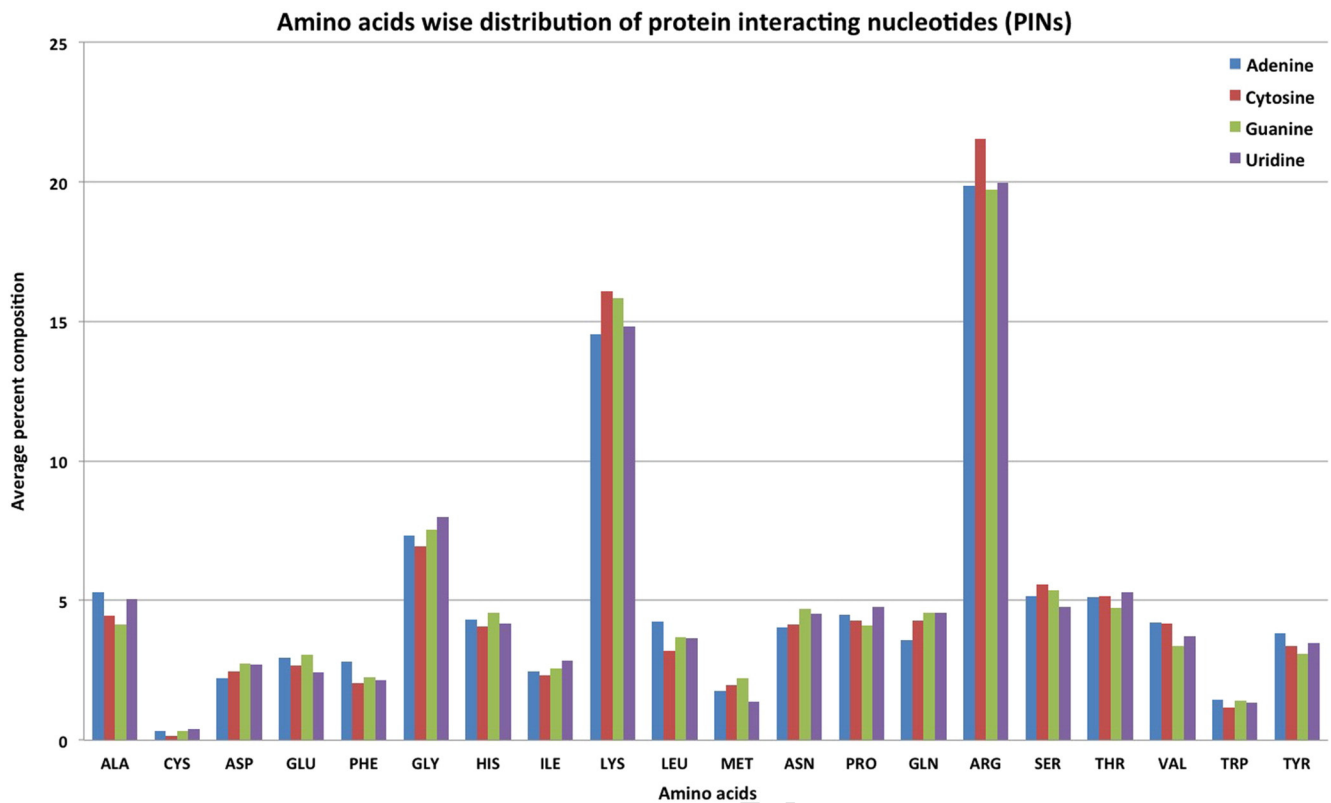


Fig. 1. Amino acids wise composition of protein interacting nucleotides.

190 calculated probability score using Eq. (5). We present score for display
 191 single digit between 0 to 9 and called probability score in this study. Dep-
 192 ending on model SVM score vary between 2.5 (around) and -2.5
 193 (around). We converted SVM score into probability score using the fol-
 194 lowing steps. First, all SVM scores of more than 1.5 were assigned 1.5
 195 and likewise less than -1.5 were assigned as -1.5 . This way all score
 196 falls between -1.5 to 1.5. Secondly, 1.5 is added to each score so
 197 score falls between 0.0 to 3.0. In order to keep the number between 0

to 9, we divide each number by 3.0 and multiplied by 9. The following
 equation is used for computing the probability score.

$$\text{Probability score} = \text{int}\left(\frac{\text{SVM score} + 1.5}{3} \times 9\right) \quad (5)$$

We used probability score in RNApin webserver instead of simple
 SVM score for each nucleotide because it is easy to display with every

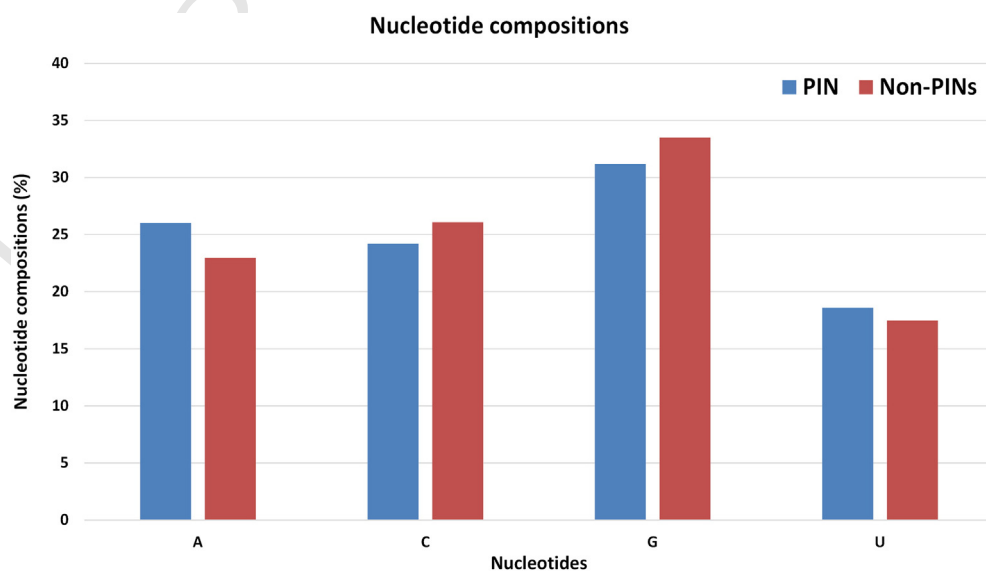


Fig. 2. Compositions of protein-interacting and non-interacting nucleotides.

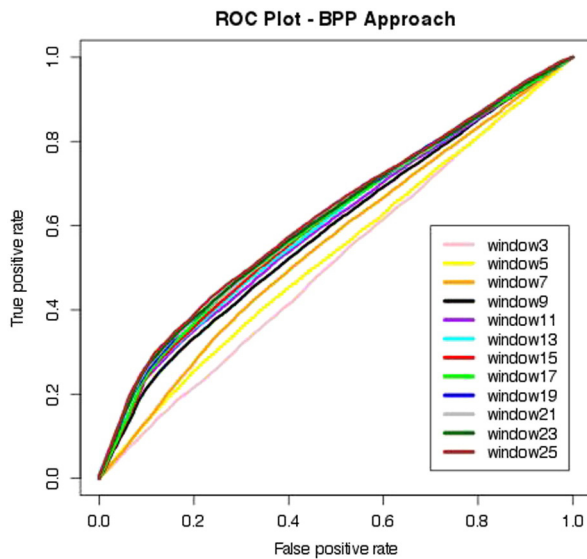


Fig. 3. ROC graph showing prediction performances of BPP approach based SVM models for 3–25 window sizes.

nucleotide of RNA sequence. The probability scores range from 0–9, where scores of 0–4 and 5–9 predicted as non-protein interacting and protein-interacting nucleotides respectively (at default 0.0 threshold level).

3. Results

3.1. Analysis of protein interacting nucleotides

Initially we extracted a total of 1546 protein-interacting RNA chains from PRIDB database [29] and used for our preliminary analysis. We analyzed amino acids wise interaction preference of different nucleotides and found that arginine, lysine and glycine were three most preferred whereas cysteine, methionine and tryptophan were non-preferred nucleotide interacting amino acids (Fig. 1). These observations agree

with previous studies on RNA–protein complexes [17,43]. We also compute preference of residues with different nucleotides but no preference was observed. Moreover, we analyzed length-wise variation of a total of 35,063 protein interacting nucleotide stretches in RNA-1546 dataset. Most of the interacting stretches (92.88%) were 1–15 nucleotides long but single, di and tri-nucleotides were most abundant. Earlier Gromiha et al. showed that 17%, 15%, 15%, 16% and 11% of binding stretches are accommodate with mono, di, tri, tetra and penta nucleotides respectively [43] whereas we found that 17%, 17%, 16%, 12%, and 9% of stretches are constituted by mono, di, tri, tetra and penta-nucleotides respectively (Supplementary Fig. S1).

We calculated nucleotide compositions and found that there is no significant difference between the protein interacting and non-interacting nucleotides (Fig. 2); these observations agree with the previous study [43]. We calculated the composition of all possible pair of di-nucleotides (Supplementary Fig. S2) and tri-nucleotides (Supplementary Fig. S3) and found that there are some differences present in the compositions.

In the past, various residue/nucleotide level prediction methods have been developed on the basis of overlapping (sliding) window pattern strategy [20,31,17]. In this, we created overlapping window patterns of different 3–25 lengths from RNA-208 dataset. A pattern is assigned protein interacting or positive if the nucleotide at its center is protein interacting otherwise it was assigned as negative or non-protein interacting. To discriminate these positive and negative patterns, we applied various approaches and developed different SVM based prediction models. All the models have been evaluated using five-fold cross validation technique.

3.2. Performance of binary profile of patterns

In the past, various biological prediction methods have been developed using binary profile of patterns (BPP) approach [31,44]. Therefore, we created binary profiles of positive and negative patterns of different window sizes (see Material and methods section). These BPPs were used as input for the SVM based machine learning. Different kernels and parameters were optimized, but prediction performance was not good. We achieved maximum 61.57% sensitivity, 54.89% specificity, 250

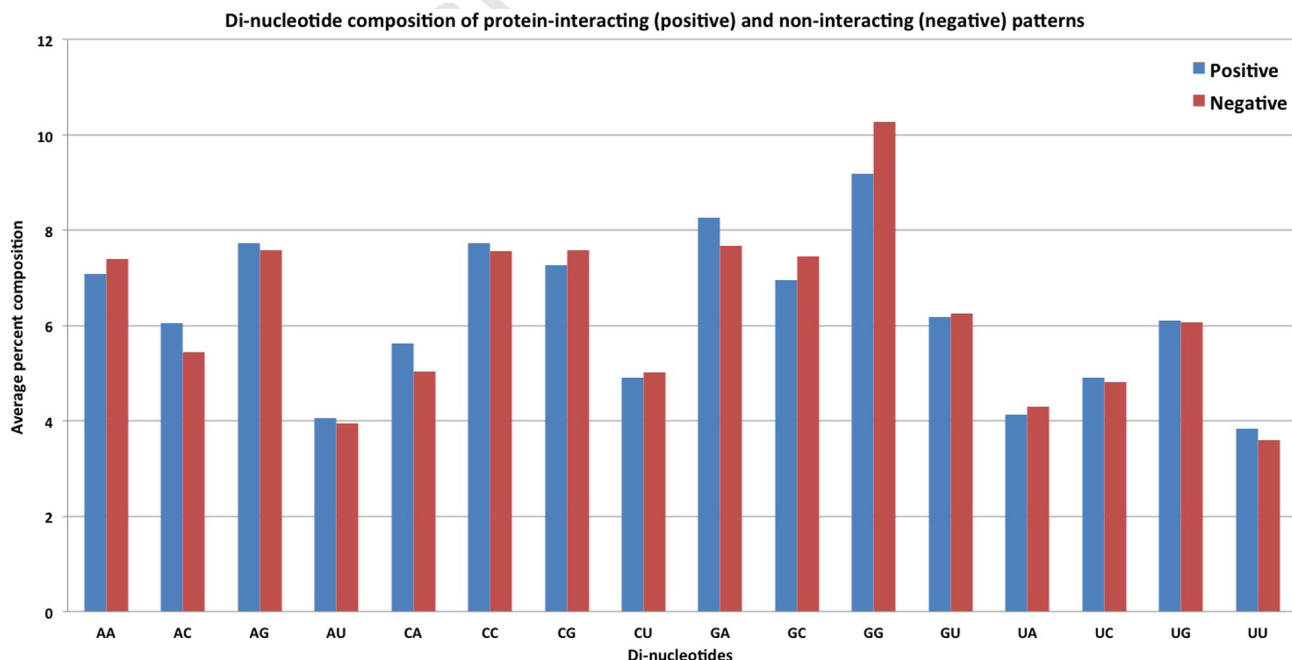


Fig. 4. Di-nucleotide composition of protein interacting (positive) and non-interacting (negative) patterns.

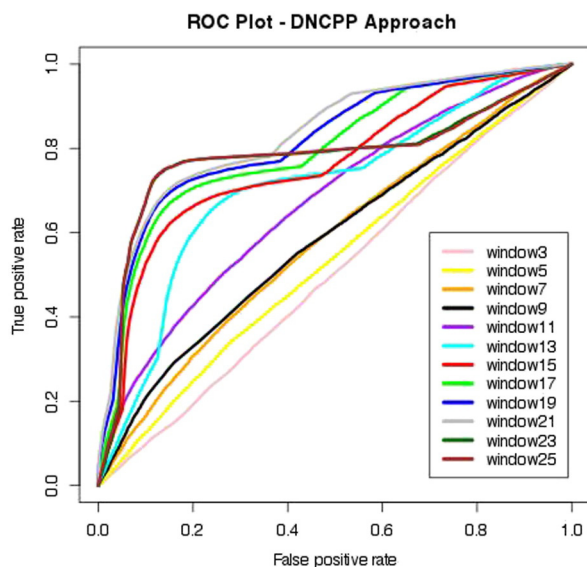


Fig. 5. ROC graph showing prediction performances of DNCPP approach based SVM models for 3–25 window sizes.

56.35% accuracy, 0.13 MCC and 0.622 AUC for window length of 25 (Fig. 3, Supplementary Table S1).

3.3. Performance of composition profile of patterns

The composition profile of patterns (CPP) can also be used for the prediction model development, when residue/nucleotide based compositional differences present between the positive and negative patterns [34,33].

3.3.1. Mono-nucleotide composition profile of patterns (MNCPP)

In the past, various prediction methods have been developed using nucleotide/amino acid composition based approach [31,45]. We calculated nucleotide compositions of the protein-interacting (positive) and non-interacting (negative) patterns and observed that there was no

nucleotide-wise preference for protein-interaction (Supplementary Fig. S4). We used these positive and negative composition profiles as input for the SVM based machine learning. As expected, all the performances were very poor and achieved only 53.69% sensitivity, 52.51% specificity, 52.76% accuracy, 0.05 MCC and 0.564 AUC for window length of 21 (Supplementary Fig. S5, Supplementary Table S2).

3.3.2. Di-nucleotide composition profile of patterns (DNCPP)

Simple mono-nucleotides composition provides information of nucleotide fraction in each pattern, whereas di-nucleotide composition provides fraction information as well as the order and neighboring nucleotide information. In DNCPP approach, we calculated di-nucleotide composition of all positive and negative patterns (Fig. 4) and used these DNCPP as SVM input. We achieved maximum 74.81% sensitivity, 76.72% specificity, 76.31% accuracy, 0.45 MCC and 0.832 AUC for window length of 21 (Fig. 5, Supplementary Table S3).

3.3.3. Tri-nucleotide composition profile of patterns (TNCPP)

Tri-nucleotide composition is more informative than di-nucleotide composition because it provides information of two neighboring nucleotides. In TNCPP approach, we calculated tri-nucleotide composition of all positive and negative patterns (Fig. 6). These TNCPPs were used as an input for SVM based machine learning. We optimized different kernels and parameters on all window sizes (3–25) and finally selected the best performing prediction model. We achieved highest 83.92% sensitivity, 84.82% specificity, 84.62% accuracy, 0.62 MCC and 0.889 AUC for window length of 19 (Fig. 7, Supplementary Table S4).

We also tried different classifiers such as NaiveBayes, NaiveBayesMultinomial, BayesNet, ComplementNaiveBayes, MultilayerPerceptron, J48, SMO, RandomForest and SMO using WEKA and achieved 0.07, 0.09, 0.10, 0.10, 0.16, 0.38, 0.46, 0.47 and 0.52 values of MCC respectively (Table 1). It means SVM^{light} based models achieved highest 0.62 MCC for predicting protein-interacting nucleotides in the RNA sequences.

4. Discussion

The RNA–protein interactions are involved in various biological processes. In order to understand and investigate those interactions, it is

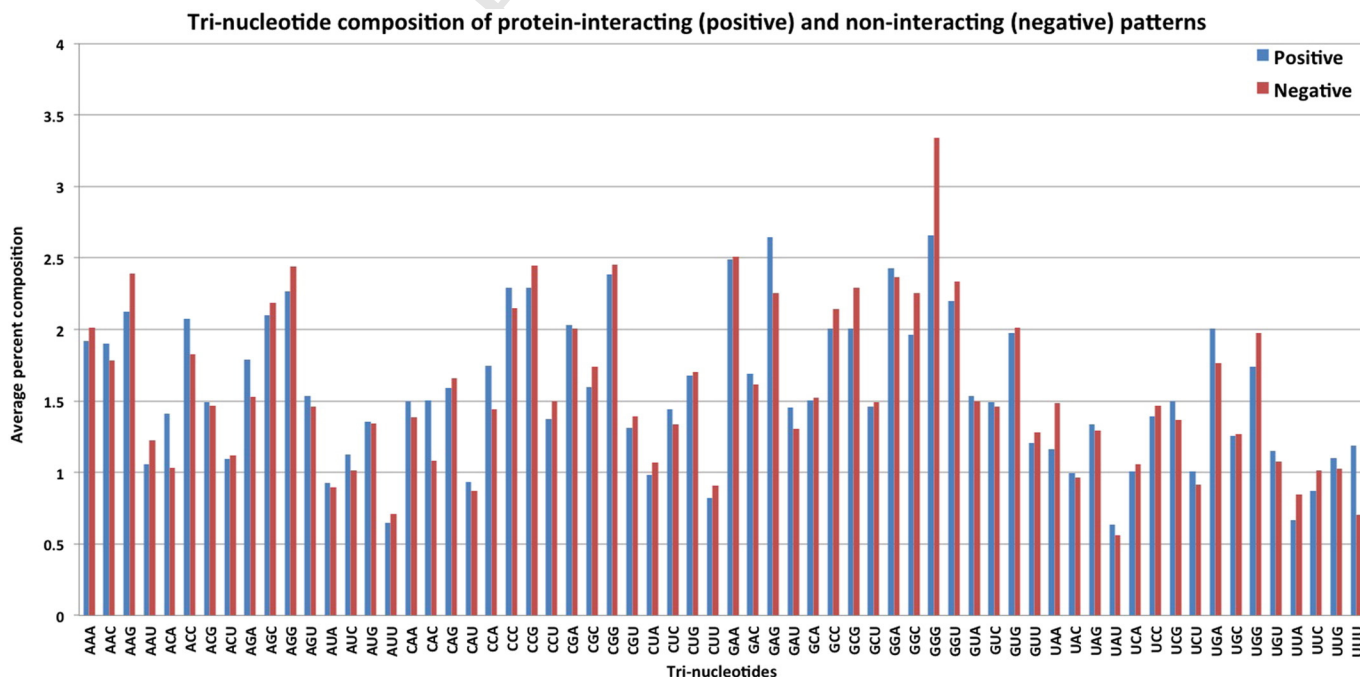


Fig. 6. Tri-nucleotide composition of protein interacting (positive) and non-interacting (negative) patterns.

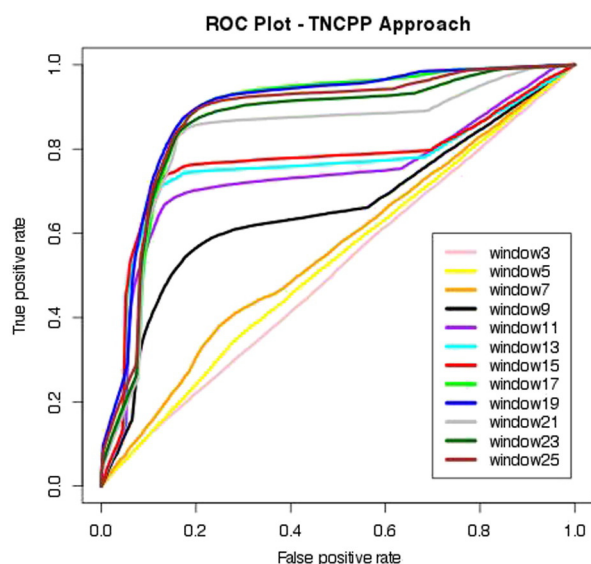


Fig. 7. ROC graph showing prediction performances of TNCPP approach based SVM models for 3–25 window sizes.

Q8 important to identify interacting amino acids and nucleotides. There are
 299 several prediction methods that have been developed to predict RNA-
 300 interacting amino acids in the protein sequences but limited method
 301 available for the prediction of interacting nucleotides in RNA sequence.
 302 We created RNA-208 dataset of 208 RNA chains from PRIDB database
 303 [29]. We calculated the RNA interaction preference of each amino acid
 304 and found that Arg, Lys and Gly are most abundant RNA-interacting nu-
 305 cleotides. Thereafter, interaction preference of each nucleotide for every
 306 amino acid was calculated and observed that there was no nucleotide-
 307 wise preference present or very little preference present e.g. cytosine
 308 slightly preferred to interact with arginine in comparison to the other
 309 nucleotides (Fig. 1). It was interesting to analyze the length of
 310 protein interacting nucleotide stretch and found that most of the
 311 interacting stretches are 1–15 nucleotides long, where single, di
 312 and tri-nucleotides were most abundant (Supplementary Fig. S1).

313 To develop a prediction tool, it is important to convert biological
 314 knowledge/information into the machine-readable numerical forms.
 315 In the past, several studies have used sliding window-based strategy
 316 to develop residue/nucleotide level prediction [20,17]. We created slid-
 317 ing window of different length and assigned window pattern as positive
 318 if the central nucleotide of the window was protein interacting other-
 319 wise assigned as negative. This assignment provided a total of 10,198
 320 positive and 36,384 negative window patterns. The next challenge is
 321 how to discriminate these positive and negative patterns efficiently.
 322 The BPP is a widely used approach for this task [44,31]. This approach
 323 provides position-wise nucleotide information of the window pattern.
 324 Therefore, we applied BPP approach, but it achieved maximum 61.57%

Table 1

t1.1 The prediction performance of different classifiers using TNCPP approach of 19-length
 t1.2 window size.
 t1.3

t1.4	Name of classifier	Sensitivity	Specificity	Accuracy	MCC
t1.5	NaiveBayes	52.47	56.35	55.50	0.07
t1.6	NaiveBayesMultinomial	49.44	61.49	58.85	0.09
t1.7	BayesNet	50.77	60.93	58.71	0.10
t1.8	ComplementNaiveBayes	41.05	70.01	63.67	0.10
t1.9	MultilayerPerceptron	54.20	64.57	62.30	0.16
t1.10	J48	55.30	84.10	77.79	0.38
t1.11	SMO	39.65	95.96	83.63	0.46
t1.12	RandomForest	78.03	76.54	76.87	0.47
t1.13	IBk	76.54	81.99	80.80	0.52
t1.14	SVM ^{light}	83.92	84.82	84.62	0.62

sensitivity, 54.89% specificity, 56.35% accuracy, 0.13 MCC and 0.622
 325 AUC for window length of 25 (Fig. 3, Supplementary Table S1). The
 326 CPP approach has been also used in the past, where it was showed
 327 that nucleotide/amino acid composition of positive and negative pat-
 328 terns can also use to discriminate these patterns [34,33]. In the
 329 MNCPP approach, performance decreased slightly compare to BPP and
 330 achieved 53.69% sensitivity, 52.51% specificity, 52.76% accuracy, 0.05
 331 MCC and 0.564 AUC for window length of 21 (Supplementary Fig. S5,
 332 Supplementary Table S2). Performance increased significantly when
 333 we applied DNCPP and achieved maximum 74.81% sensitivity, 76.72%
 334 specificity, 76.31% accuracy, 0.45 MCC and 0.832 AUC for window length
 335 of 21 (Fig. 5, Supplementary Table S3). It may be because there were dif-
 336 ferent nucleotides preferred in the positive and negative patterns. We
 337 observed that AC, CA, GA and UU di-nucleotide preferred in positive pat-
 338 terns, whereas AA, CG, GC and GG preferred in negative patterns (Fig. 4).
 339 Finally, TNCPP achieved highest 83.92% sensitivity, 84.82% specificity,
 340 84.62% accuracy, 0.62 MCC and 0.889 AUC for window length of 19
 341 (Fig. 7, Supplementary Table S4). Here also tri-nucleotide wise prefer-
 342 ences were present, where ACA, ACC, AGA, CAC, CCA, GAG, UGA and
 343 UUU tri-nucleotides preferred in positive patterns, whereas AAG, AGG,
 344 CCG, CGC, GCG, GGC, GGG, GGU, UAA, UGG and UUC preferred in nega-
 345 tive patterns (Fig. 6).
 346

In the present scenario, prediction of protein interacting nucleotides
 347 is in the primitive stage. We tried various approaches and achieved rea-
 348 sonable performance, but this problem requires more attention and in-
 349 formation, in order to develop an efficient prediction model. The
 350 present method has many limitations due to limited dataset availability
 351 and criterion to determine protein interacting and non-interacting nu-
 352 cleotides. We used 5.0 Å as a cutoff distance because in the past various
 353 methods have been used in this criterion for selecting RNA-interacting
 354 residues in proteins [30] but this is not solely a correct criterion. Recent-
 355 ly, pseudo k-tuple nucleotide composition (PseKNC) based approach
 356 also proposed for different nucleotide related problems [46,47] and
 357 our approach can be extended in future works. Additionally, there are
 358 sequence-independent bindings also present in the RNA–protein inter-
 359 action; therefore, it is important to solve these issues in the future. We
 360 hope that *RNApin* method will be useful for the RNA biologist in order
 361 to identify protein interacting nucleotides in RNA sequences.
 362

5. Conclusion

In this study, we tried various approaches for the prediction of PINs.
 364 We optimized different window sizes, SVM parameters and kernels. Fi-
 365 nally we found that tri-nucleotide wise compositional differences were
 366 present between positive and negative patterns and TNCPP approach
 367 was most efficient to discriminate PINs and non-PINs.
 368

RNApin web-server

We implemented SVM prediction model in a web-server called
 370 *RNApin*. The *RNApin* is user-friendly and freely available from [http://](http://crdd.osdd.net/raghava/rnapin/)
 371 crdd.osdd.net/raghava/rnapin/ web-address. We have provided our
 372 dataset 'RNA-208' in the supplementary file 2 (RNA-208.txt) and also
 373 RNA-1546 is accessible from our *RNApin* webserver ([http://crdd.osdd.](http://crdd.osdd.net/raghava/rnapin/dataset.php)
 374 [net/raghava/rnapin/dataset.php](http://crdd.osdd.net/raghava/rnapin/dataset.php)).
 375

Author's contributions

BP created dataset, optimized and developed the SVM models. BP
 377 also created the backend web server and the front end user interface.
 378 GPSR conceived the project, coordinated it and refined the manuscript
 379 drafted by BP. Both authors have read and approved the final draft of
 380 the manuscript.
 381

382 **Competing interests**

383 The authors declare that they have no competing interests.

384 **Acknowledgments**

385 Authors are thankful to funding agencies Council of Scientific and Industrial Research (project OSDD and GENESIS BSC0121) and Department
386 of Biotechnology (project BTISNET), Govt. of India. This report has Institute of Microbial Technology (IMTECH) communication no. 026/2013.
387

389 **Appendix A. Supplementary data**

390 Supplementary data to this article can be found online at <http://dx.doi.org/10.1016/j.ygeno.2015.01.005>.
391

392 **References**

- 393 [1] D.E. Draper, Themes in RNA–protein recognition, *J. Mol. Biol.* 293 (1999) 255–270. <http://dx.doi.org/10.1006/jmbi.1999.2991>.
394
395 [2] N. Morozova, J. Allers, J. Myers, Y. Shamoo, Protein–RNA interactions: exploring
396 binding patterns with a three-dimensional superposition analysis of high resolution
397 structures, *Bioinformatics* 22 (2006) 2746–2752. <http://dx.doi.org/10.1093/bioinformatics/btl470>.
398
399 [3] J. Iwakiri, H. Tateishi, A. Chakraborty, P. Patil, N. Kenmochi, Dissecting the protein–
400 RNA interface: the role of protein surface shapes and RNA secondary structures in
401 protein–RNA recognition, *Nucleic Acids Res.* 40 (2012) 3299–3306. <http://dx.doi.org/10.1093/nar/gkr1225>.
402
403 [4] A.C. Cheng, W.W. Chen, C.N. Fuhrmann, A.D. Frankel, Recognition of nucleic acid
404 bases and base-pairs by hydrogen bonding to amino acid side-chains, *J. Mol. Biol.*
405 327 (2003) 781–796 (<http://www.ncbi.nlm.nih.gov/pubmed/12654263>, accessed
406 February 01, 2013).
407 [5] A.M. Khalil, J.L. Rinn, RNA–protein interactions in human health and disease, *Semin.*
408 *Cell Dev. Biol.* 22 (2011) 359–365. <http://dx.doi.org/10.1016/j.semcdb.2011.02.016>.
409 [6] J.C. Darnell, C.E. Fraser, O. Mostovetsky, G. Stefani, T.A. Jones, S.R. Eddy, et al., Kissing
410 complex RNAs mediate interaction between the fragile-X mental retardation protein
411 KH2 domain and brain polyribosomes, *Genes Dev.* 19 (2005) 903–918. <http://dx.doi.org/10.1101/gad.1276805>.
412
413 [7] F. Bolognani, N.I. Perrone-Bizzozero, RNA–protein interactions and control of mRNA
414 stability in neurons, *J. Neurosci. Res.* 86 (2008) 481–489. <http://dx.doi.org/10.1002/jnr.21473>.
415
416 [8] S.J. Kolb, D.J. Battle, G. Dreyfuss, Molecular functions of the SMN complex, *J. Child*
417 *Neurol.* 22 (2007) 990–994. <http://dx.doi.org/10.1177/0883073807305666>.
418 [9] R.N. Kanadia, J. Shin, Y. Yuan, S.G. Beattie, T.M. Wheeler, C.A. Thornton, et al., Reversal
419 of RNA missplicing and myotonia after muscleblind overexpression in a mouse
420 poly(CUG) model for myotonic dystrophy, *Proc. Natl. Acad. Sci. U. S. A.* 103 (2006)
421 11748–11753. <http://dx.doi.org/10.1073/pnas.0604970103>.
422 [10] C.K. Iwahashi, D.H. Yasui, H.-J. An, C.M. Greco, F. Tassone, K. Nannen, et al., Protein
423 composition of the intranuclear inclusions of FXTAS, *Brain* 129 (2006) 256–271. <http://dx.doi.org/10.1093/brain/awh650>.
424
425 [11] L.M. Hellman, M.G. Fried, Electrophoretic mobility shift assay (EMSA) for detecting
426 protein–nucleic acid interactions, *Nat. Protoc.* 2 (2007) 1849–1861. <http://dx.doi.org/10.1038/nprot.2007.249>.
427
428 [12] J. Ule, K. Jensen, A. Mele, R.B. Darnell, CLIP: a method for identifying protein–RNA
429 interaction sites in living cells, *Methods* 37 (2005) 376–386. <http://dx.doi.org/10.1016/j.ymeth.2005.07.018>.
430
431 [13] A. Günzl, Z. Palfi, A. Bindereif, Analysis of RNA–protein complexes by
432 oligonucleotide-targeted RNase H digestion, *Methods* 26 (2002) 162–169. [http://dx.doi.org/10.1016/S1046-2023\(02\)00019-1](http://dx.doi.org/10.1016/S1046-2023(02)00019-1).
433
434 [14] J.D. Keene, J.M. Komisarow, M.B. Friedersdorf, RIP-Chip: the isolation and identification
435 of mRNAs, microRNAs and protein components of ribonucleoprotein complexes
436 from cell extracts, *Nat. Protoc.* 1 (2006) 302–307. <http://dx.doi.org/10.1038/nprot.2006.47>.
437
438 [15] S.A. Tenenbaum, P.J. Lager, C.C. Carson, J.D. Keene, Ribonomics: identifying
439 mRNA subsets in mRNP complexes using antibodies to RNA-binding proteins and
440 genomic arrays, *Methods* 26 (2002) 191–198. [http://dx.doi.org/10.1016/S1046-2023\(02\)00022-1](http://dx.doi.org/10.1016/S1046-2023(02)00022-1).
441
442 [16] D.L. Beach, J.D. Keene, Ribotrap: targeted purification of RNA-specific RNPs from cell
443 lysates through immunoaffinity precipitation to identify regulatory proteins and
444 RNAs, *Methods Mol. Biol.* 419 (2008) 69–91. http://dx.doi.org/10.1007/978-1-59745-033-1_5.
445
446 [17] M. Kumar, M.M. Gromiha, G.P.S. Raghava, Prediction of RNA binding sites in a protein
447 using SVM and PSSM profile, *Proteins* 71 (2008) 189–194. <http://dx.doi.org/10.1002/prot.21677>.
448
449 [18] M. Terribilini, J.D. Sander, J.-H. Lee, P. Zaback, R.L. Jernigan, V. Honavar, et al.,
450 RNABindR: a server for analyzing and predicting RNA-binding sites in proteins,
451 *Nucleic Acids Res.* 35 (2007) W578–W584. <http://dx.doi.org/10.1093/nar/gkm294>.
452
453 [19] L. Wang, C. Huang, M.Q. Yang, J.Y. Yang, BindN+ for accurate prediction of DNA and
454 RNA-binding residues from protein sequence features, *BMC Syst. Biol.* 4 (Suppl. 1)
455 (2010) S3. <http://dx.doi.org/10.1186/1752-0509-4-S1-S3>.

- [20] R.V. Spriggs, Y. Murakami, H. Nakamura, S. Jones, Protein function annotation from
456 sequence: prediction of residues interacting with RNA, *Bioinformatics* 25 (2009)
457 1492–1497. <http://dx.doi.org/10.1093/bioinformatics/btp257>.
458
459 [21] S. Choi, K. Han, Predicting protein-binding RNA nucleotides using the feature-
460 based removal of data redundancy and the interaction propensity of nucleotide
461 triplets, *Comput. Biol. Med.* 43 (2013) 1687–1697. <http://dx.doi.org/10.1016/j.combiomed.2013.08.011>.
462
463 [22] S.-H. Guo, E.-Z. Deng, L.-Q. Xu, H. Ding, H. Lin, W. Chen, et al., iNuc-PseKNC: a
464 sequence-based predictor for predicting nucleosome positioning in genomes with
465 pseudo k-tuple nucleotide composition, *Bioinformatics* 30 (2014) 1522–1529. <http://dx.doi.org/10.1093/bioinformatics/btu083>.
466
467 [23] W. Chen, P.-M. Feng, E.-Z. Deng, H. Lin, K.-C. Chou, iTIS-PseTNC: a sequence-based
468 predictor for identifying translation initiation site in human genes using pseudo tri-
469 nucleotide composition, *Anal. Biochem.* 462 (2014) 76–83. <http://dx.doi.org/10.1016/j.ab.2014.06.022>.
470
471 [24] W.-R. Qiu, X. Xiao, K.-C. Chou, iRSpot-TNCPseAAC: identify recombination spots
472 with trinucleotide composition and pseudo amino acid components, *Int. J. Mol.*
473 *Sci.* 15 (2014) 1746–1766. <http://dx.doi.org/10.3390/ijms15021746>.
474
475 [25] K.-C. Chou, Some remarks on protein attribute prediction and pseudo amino acid
476 composition, *J. Theor. Biol.* 273 (2011) 236–247. <http://dx.doi.org/10.1016/j.jtbi.2010.12.024>.
477
478 [26] H. Lin, E.-Z. Deng, H. Ding, W. Chen, K.-C. Chou, iPro54-PseKNC: a sequence-based
479 predictor for identifying sigma-54 promoters in prokaryote with pseudo k-tuple nucleotide
480 composition, *Nucleic Acids Res.* 42 (2014) 12961–12972. <http://dx.doi.org/10.1093/nar/gku1019>.
481
482 [27] B. Liu, F. Liu, L. Fang, X. Wang, K.-C. Chou, repDNA: a Python package to generate
483 various modes of feature vectors for DNA sequences by incorporating user-
484 defined physicochemical properties and sequence-order effects, *Bioinformatics* (2014)
485 <http://dx.doi.org/10.1093/bioinformatics/btu820>.
486
487 [28] W. Chen, X. Zhang, J. Brooker, H. Lin, L. Zhang, K.-C. Chou, PseKNC-General: a cross-
488 platform package for generating various modes of pseudo nucleotide compositions,
489 *Bioinformatics* 31 (2014) 119–120. <http://dx.doi.org/10.1093/bioinformatics/btu602>.
490
491 [29] B.A. Lewis, R.R. Walia, M. Terribilini, J. Ferguson, C. Zheng, V. Honavar, et al., PRIDB: a
492 protein–RNA interface database, *Nucleic Acids Res.* 39 (2011) D277–D282. <http://dx.doi.org/10.1093/nar/gkq1108>.
493
494 [30] R.R. Walia, C. Caragea, B.A. Lewis, F. Towfic, M. Terribilini, Y. El-Manzalawy, et al., Protein–RNA
495 interface residue prediction using machine learning: an assessment of the state of the art, *BMC Bioinf.* 13 (2012) 89. <http://dx.doi.org/10.1186/1471-2105-13-89>.
496
497 [31] F. Ahmed, G.P.S. Raghava, Designing of highly effective complementary and mis-
498 matching siRNAs for silencing a gene, *PLoS ONE* 6 (2011) e23443. <http://dx.doi.org/10.1371/journal.pone.0023443>.
499
500 [32] B. Panwar, G.P. Raghava, Prediction of uridine modifications in tRNA sequences, *BMC Bioinf.* 15 (2014) 326. <http://dx.doi.org/10.1186/1471-2105-15-326>.
501
502 [33] H.R. Ansari, G.P. Raghava, Identification of conformational B-cell epitopes in an antigen
503 from its primary sequence, *Immunome Res.* 6 (2010) 6. <http://dx.doi.org/10.1186/1745-7580-6-6>.
504
505 [34] S. Agarwal, N.K. Mishra, H. Singh, G.P.S. Raghava, Identification of mannose
506 interacting residues using local composition, *PLoS ONE* 6 (2011) e24039. <http://dx.doi.org/10.1371/journal.pone.0024039>.
507
508 [35] V.N. Vapnik, An overview of statistical learning theory, *IEEE Trans. Neural Netw.* 10
509 (1999) 988–999. <http://dx.doi.org/10.1109/72.788640>.
510
511 [36] T. Joachims, Making large-scale SVM learning practical, *Adv. Kernel Methods Support*
512 *Vector Learn* 1999, 169–184. <http://dx.doi.org/10.1109/ICML.2009.5274151>.
513
514 [37] M. Hall, E. Frank, G. Holmes, B. Pfahringer, P. Reutemann, I.H. Witten, The WEKA
515 data mining software: an update, *SIGKDD Explor.* 11 (2009) 10–18. <http://dx.doi.org/10.1145/1656274.1656278>.
516
517 [38] K.C. Chou, C.T. Zhang, Prediction of protein structural classes, *Crit. Rev. Biochem.*
518 *Mol. Biol.* 30 (1995) 275–349. <http://dx.doi.org/10.3109/10409239509083488>.
519
520 [39] K.-C. Chou, H.-B. Shen, Cell-PLOC: a package of web servers for predicting subcellular
521 localization of proteins in various organisms, *Nat. Protoc.* 3 (2008) 153–162. <http://dx.doi.org/10.1038/nprot.2007.494>.
522
523 [40] B. Panwar, S. Gupta, G.P. Raghava, Prediction of vitamin interacting residues in a vitamin
524 binding protein using evolutionary information, *BMC Bioinf.* 14 (2013) 44. <http://dx.doi.org/10.1186/1471-2105-14-44>.
525
526 [41] B. Panwar, G.P.S. Raghava, Prediction and classification of aminoacyl tRNA synthetases
527 using PROSITE domains, *BMC Genomics* 11 (2010) 507. <http://dx.doi.org/10.1186/1471-2164-11-507>.
528
529 [42] B. Panwar, A. Arora, G.P.S. Raghava, Prediction and classification of ncRNAs using
530 structural information, *BMC Genomics* 15 (2014) 127. <http://dx.doi.org/10.1186/1471-2164-15-127>.
531
532 [43] M.M. Gromiha, K. Yokota, K. Fukui, Understanding the recognition mechanism of
533 protein–RNA complexes using energy based approach, *Curr. Protein Pept. Sci.* 11
534 (2010) 629–638 (<http://www.ncbi.nlm.nih.gov/pubmed/20887255>, accessed
535 November 30, 2014).
536
537 [44] J.S. Chauhan, N.K. Mishra, G.P.S. Raghava, Identification of ATP binding residues of a
538 protein from its primary sequence, *BMC Bioinf.* 10 (2009) 434. <http://dx.doi.org/10.1186/1471-2105-10-434>.
539
540 [45] B. Panwar, G.P.S. Raghava, Predicting sub-cellular localization of tRNA synthetases
541 from their primary structures, *Amino Acids* 42 (2012) 1703–1713. <http://dx.doi.org/10.1007/s00726-011-0872-8>.
542
543 [46] W. Chen, T.-Y. Lei, D.-C. Jin, H. Lin, K.-C. Chou, PseKNC: a flexible web server for
544 generating pseudo K-tuple nucleotide composition, *Anal. Biochem.* 456 (2014) 53–60. <http://dx.doi.org/10.1016/j.ab.2014.04.001>.
545
546 [47] W. Chen, P.-M. Feng, H. Lin, K.-C. Chou, iRSpot-PseDNC: identify recombination
547 spots with pseudo dinucleotide composition, *Nucleic Acids Res.* 41 (2013) e68. <http://dx.doi.org/10.1093/nar/gks1450>.